(Received 18 September 2024, Accepted 29 October 2024, Scheduled 11 November 2024)

A Low-Profile Single-Layered Wideband Combinational Reconfigurable Antenna for 4G and 5G Applications

Sweta Agarwal[1], Akanksha Singh[2], and Manoj Kumar Meshram[1,*]

[1]*Department of Electronics Engineering, Indian Institute of Technology (BHU), Varanasi, India*
[2]*Noida Institute of Engineering and Technology, Greater Noida, India*

ABSTRACT: A single-layered monopole wideband combinational reconfigurable antenna for 4G and 5G applications is presented in this paper. Coplanar waveguide (CPW) feeding method is utilized to get a single-layered structure. The three characteristics of this antenna are reconfigurable: frequency, polarization, and radiation pattern. This antenna consists of a parasitic element attached to a rectangular ring antenna. An RF-PIN diode is used to connect this parasitic element to the ring antenna. Additionally, two parasitic elements are connected to the ground plane of the proposed antenna via a pair of RF-PIN diodes. The suggested antenna functions in seven distinct states using these three RF-PIN diodes. The suggested antenna operates at frequencies of 3.24–3.52 GHz, 2.78–2.94 GHz, and 2.54–2.9 GHz with an omnidirectional radiation pattern in states 1, 2, and 5. In states 3 and 4, it has an end-fire radiation pattern in the left and right directions of the proposed antenna, covering a wide frequency band of 2.47–3.57 GHz. Lastly, the suggested antenna operates in dual bands at frequencies of 2.49–2.9 GHz and 3.6–3.76 GHz in states 6 and 7. It offers reconfigurability of polarization at the higher band. The suggested antenna is made of glass epoxy FR-4 material. For verification of the suggested antenna, the prototype is designed and tested. The simulated and experimental results agree quite well.

1. INTRODUCTION

Using wireless technology is essential to the progress of civilization in the modern day. As a result, the field of antenna technology has advanced quickly. The demand for flexible and versatile antenna systems has increased significantly as a result of the ongoing development of wireless communication technologies like 4G and 5G. Reconfigurable antennas have emerged as a potential solution, allowing for dynamic changes to their properties to accommodate various communication standards and applications. Reconfigurable antennas have the benefit of being able to adapt to changing circumstances and user needs. By adjusting parameters such as resonant frequency, polarization, and radiation pattern, a singular reconfigurable antennas can successfully eliminate the requirement for several conventional antennas, making the system as a whole lighter, more compact, and less complicated. In the context of 4G and 5G networks, where the increasing demand for bandwidth, data rates, and seamless connectivity necessitates deploying flexible and effective antenna systems [1], this feature shows substantial benefits. Modern reconfigurable antenna design has advanced largely because of advances in actuation technologies and materials, such as PIN diodes, varactor diodes, and microelectromechanical systems (MEMSs).

For different wireless standards, there is plenty of literature available on single-parameter reconfigurability, including frequency [2–7], radiation pattern [8–13], and polarisation [14–17]. These antennas can only have one parameter, making them insufficient for the use with 4G and 5G networks. Researchers are working on hybrid or combination reconfigurable antennas to address these issues. This indicates that many characteristics, such as frequency and radiation pattern [18–21], frequency and polarisation [22–24], and radiation pattern and polarisation [25], can be changed in a single antenna. Certain finding can be adjusted in terms of frequency, radiation pattern, and polarisation [26, 27]. Nevertheless, these antennas have a complex structure and a lot of switching components. CPW-fed approach is one of the ways to simplify the structure and lower the cost of the antenna [28].

The purpose of the suggested work is to address the aforementioned issues. A CPW-fed combination reconfigurable antenna with all three characteristics is included in the proposed antenna and can be reconfigured over the whole S-band. Wide bandwidth and reduced circuit complexity are two benefits of CPW-fed antennas [28]. With just three RF-PIN diodes needed to cover 4G and 5G applications, the structure is in low profile and simple to integrate into any application. 2.52–2.60 GHz for 4G (2.5 GHz), 3.31–3.46 GHz for 5G (3.4 GHz [n77 and n78]), and 3.66–3.72 GHz for 5G (3.7 GHz [n77 and n78]) ranges are the bands for which this antenna is useful.

The proposed antenna has the following outcomes:

(i) A single-layered antenna is reconfigurable in all three properties of antenna frequency, radiation pattern, and polarization with the lowest number of diodes.

(ii) 4G and 5G applications can benefit from this recommended antenna. It covers the 5G band in a state of operation (state 1), the 4G band independently in state 5, and the 4G and 5G combination in states 6 and 7.

* Corresponding author: Manoj Kumar Meshram (mkmeshram.ece@iitbhu.ac.in).

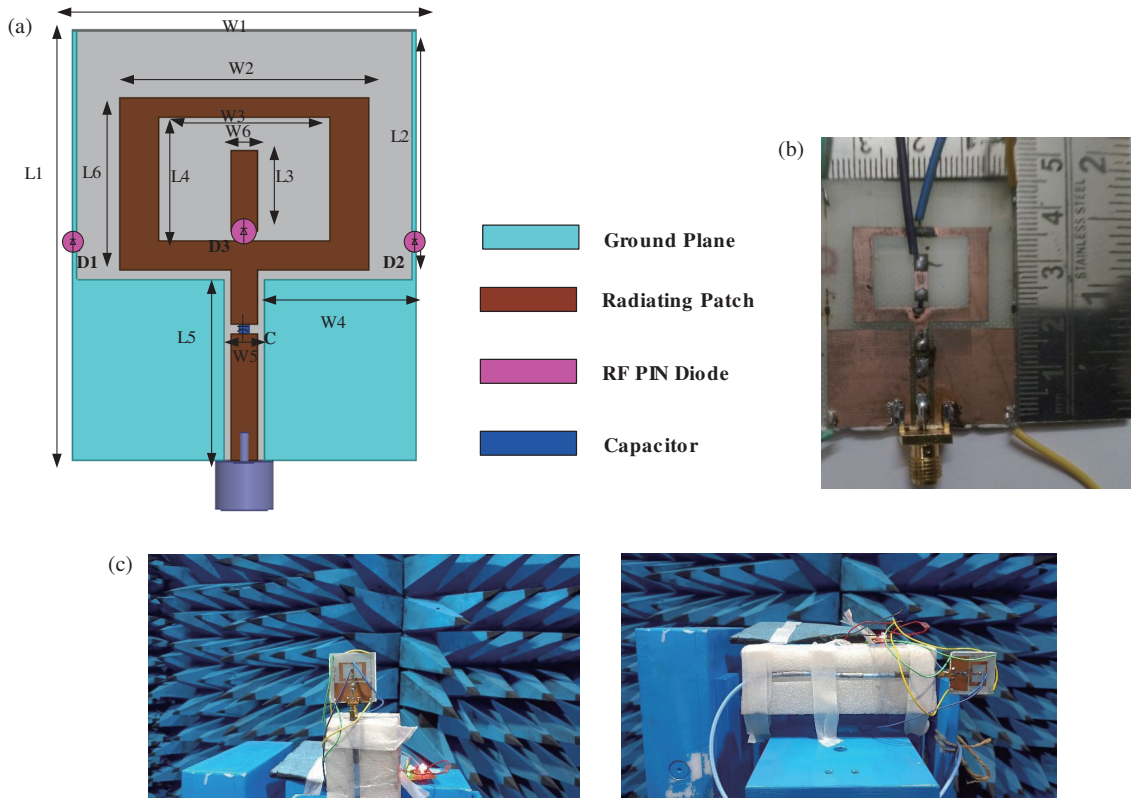

FIGURE 1. (a) Proposed antenna geometry. (b) Fabricated antenna prototype. (c) Measurement setup of proposed antenna.

(iii) All three forms of reconfigurability can be achieved with the proposed antenna without needing a complicated mechanism.

(iv) To the best of the authors' knowledge, this is the first time a combinational reconfigurable antenna having reconfigurability in three properties frequency, polarization, and radiation pattern based on CPW has been suggested.

(v) The suggested antenna is small, lightweight, and simple to use.

2. ANTENNA DESIGN METHODOLOGY AND WORKING PRINCIPLE

2.1. Proposed Antenna Geometry

A single-layer FR-4 substrate $\varepsilon_r = 4.4$, $\tan\delta = 0.02$) with a thickness of 1.6 mm is used in this design of the recommended antenna for 4G and 5G applications. A 0.035-mm thick copper material with a conductivity of 5.96×10^7 S/m is employed. The combinational reconfigurable antenna (CRA) is shown in Fig. 1 to three parameters: polarization, radiation pattern, and frequency. Table 1 displays the CRA's optimal dimensions. Initially, a rectangular ring microstrip antenna is designed. Equations (1)–(4) [29] are used for the initial design.

$$\varepsilon_{reff} = \frac{\varepsilon_r + 1}{2} + \frac{\varepsilon_r - 1}{2}\left(1 + 12\frac{h}{W}\right)^{-0.5} \quad (1)$$

TABLE 1. Proposed antenna-optimized dimensions.

Parameter	Dimensions (mm)	Parameter	Dimensions (mm)
$L1$	45	$W1$	36
$L2$	22	$W2$	26
$L3$	9	$W3$	18
$L4$	13	$W4$	15.4
$L5$	19	$W5$	2.8
$L6$	18	$W6$	2.8

$$f_0 = \frac{c}{2L\sqrt{\varepsilon_{reff}}} \quad (2)$$

$$L = \frac{c}{2f_0\sqrt{\varepsilon_{reff}}} - 2\Delta L \quad (3)$$

$$\Delta L = 0.412h\frac{(\varepsilon_{reff}+0.3)\left(\frac{W}{h}+0.264\right)}{(\varepsilon_{reff}-0.258)\left(\frac{W}{h}+0.8\right)} \quad (4)$$

W is the width of an outer ring, c the speed of light in a vacuum, and L the length of the ring's outer perimeter. f_0 is the resonant frequency, and ΔL is the extension of the length due to the fringing effect at the edges of the patch. Standard design equations for rectangular patch antennas can be modified for a ring structure by adjusting the perimeter and area.

A parasitic element is present in the rectangular ring antenna of the proposed antenna, and two parallel parasitic elements are present in the ground plane. The RF-PIN diode (D3) connects the parasitic element to the rectangular ring antenna, and

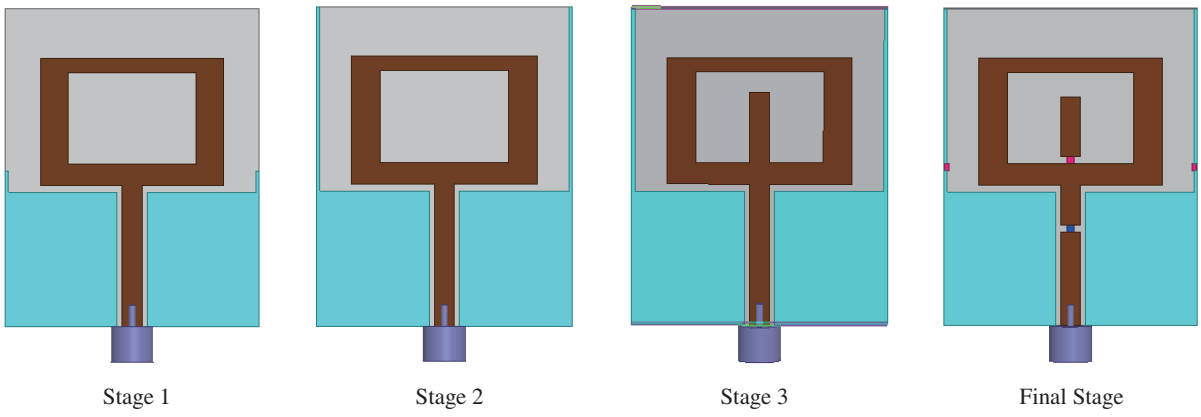

FIGURE 2. Evolution of antenna geometry.

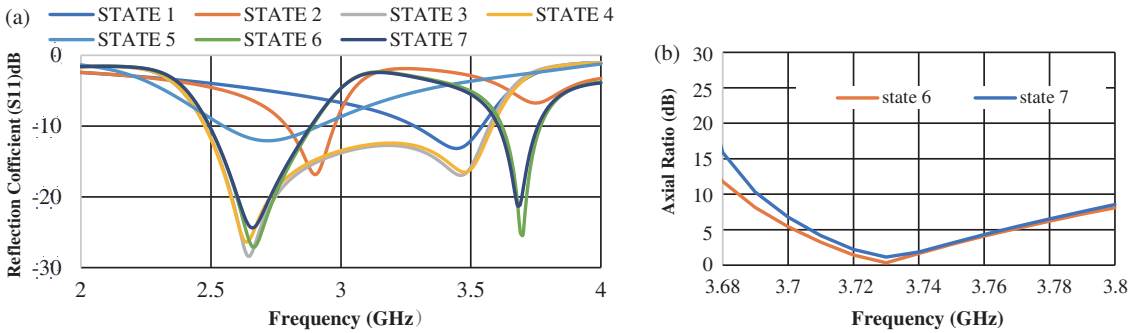

FIGURE 3. Various states of operation of the proposed antenna (a) Reflection Coefficient (S11) (b) Axial Ratio.

two RF-PIN diodes (D1 and D2) provide the connection of two parallel parasitic elements to the ground plane. A capacitor of 50 pF is used in the feed line to block the DC supply. The proposed antenna is designed using the coplanar waveguide fed (CPW) technique.

$$k' = \sqrt{1-k^2} \tag{5}$$

$$k_1 = \frac{S_c}{S_c+2W} \tag{6}$$

$$k_2 = \frac{sinh(\pi a/2h)}{sinh(\pi b/2h)} \tag{7}$$

$$\frac{K(k)}{K'(k)} = \begin{cases} \dfrac{\pi}{\ln\left[\dfrac{2\left(1+\sqrt{k'}\right)}{1-\sqrt{k'}}\right]} & (0 \le k \le 0.707) \\ \dfrac{\ln\left[\dfrac{2\left(1+\sqrt{k'}\right)}{1-\sqrt{k'}}\right]}{\pi} & (0.707 \le k \le 1) \end{cases} \tag{8}$$

$$\varepsilon_{eff} = 1 + \frac{\varepsilon_r - 1}{2} \frac{K(k_2)}{K'(k_2)} \frac{K'(k_1)}{K(k_1)} \tag{9}$$

$$Z_{ocp} = \frac{30\pi}{\sqrt{\varepsilon_{eff}}} \frac{K'(k_1)}{K(k_1)} \tag{10}$$

$$k = \frac{c}{b}\sqrt{\frac{b^2-a^2}{c^2-a^2}} \tag{11}$$

Equations (5)–(11) [30] can be used to determine the characteristic impedance of a symmetrical double-strip CPW line on a substrate with a limited thickness. Different parameters in the given equations are explained as follows: $Zocp$ is the characteristic impedance of the CPW line, Sc the width of the central conductor, W the separation between the central conductor and ground plane on two sides, h the thickness of the substrate, and ε_r the relative dielectric constant of the substrate. $K(k)$ is described as the elliptical integral of first order with argument k or the complementary argument k', where a, b, and c are the width of the feed line, the separation of the feed line from centre, and the total width of the ground plane, respectively.

2.2. Evolution of Geometry

Figure 2 displays the CRA's systematic development. As seen in Fig. 2(a), a straightforward monopole rectangular ring antenna is considered in the first design phase using the CPW-fed approach. Following that, as seen in Fig. 2(b), two parasitic elements of size $22 \times 0.5\,\text{mm}^2$ were added to the ground during the second phase of design, changing the ground's size. In the third phase of the design, a parasitic element of size $9 \times 2.8\,\text{mm}^2$ is positioned in the centre of the rectangular ring antenna to achieve the polarisation reconfigurability requirement, as illustrated in Fig. 2(c). As illustrated in Fig. 2(d), three parasitic elements are linked to the ground plane and the rectangular ring

TABLE 2. Various states of operation of proposed CRA.

Operating State	D1	D2	D3	Frequency covered (GHz)	Radiation Pattern	Condition of Reconfigurability
State 1	OFF	OFF	OFF	3.24–3.52	Omnidirectional	Frequency
State 2	OFF	OFF	ON	2.78–2.94	Omni-directional	Frequency
State 3	OFF	ON	OFF	2.47–3.57	Directional (left hand end-fire)	Radiation Pattern
State 4	ON	OFF	ON	2.47–3.57	Directional (right hand end-fire)	Radiation Pattern
State 5	ON	ON	OFF	2.54–2.9	Omni-directional	Frequency
State 6	ON	OFF	ON	2.49–2.9/3.6–3.76 (Dual band)	Directional (lower frequency)/ end-fire (higher frequency)	Frequency, Radiation Pattern and Polarization (RHCP)
State 7	OFF	ON	ON	2.49–2.9/3.6–3.76 (Dual Band)	Directional (lower frequency)/ end-fire (higher frequency)	Frequency, Radiation Pattern and Polarization (LHCP)

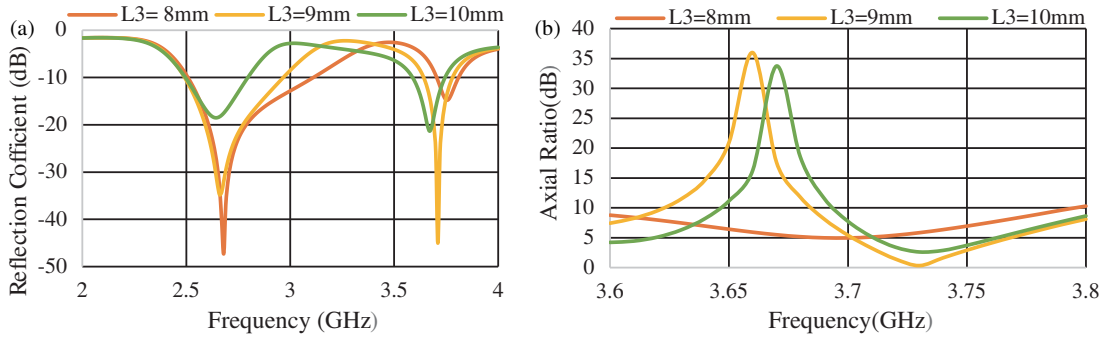

FIGURE 4. Variation in reflection coefficient (S_{11}) and axial ratio with $L3$ in states 6 and 7.

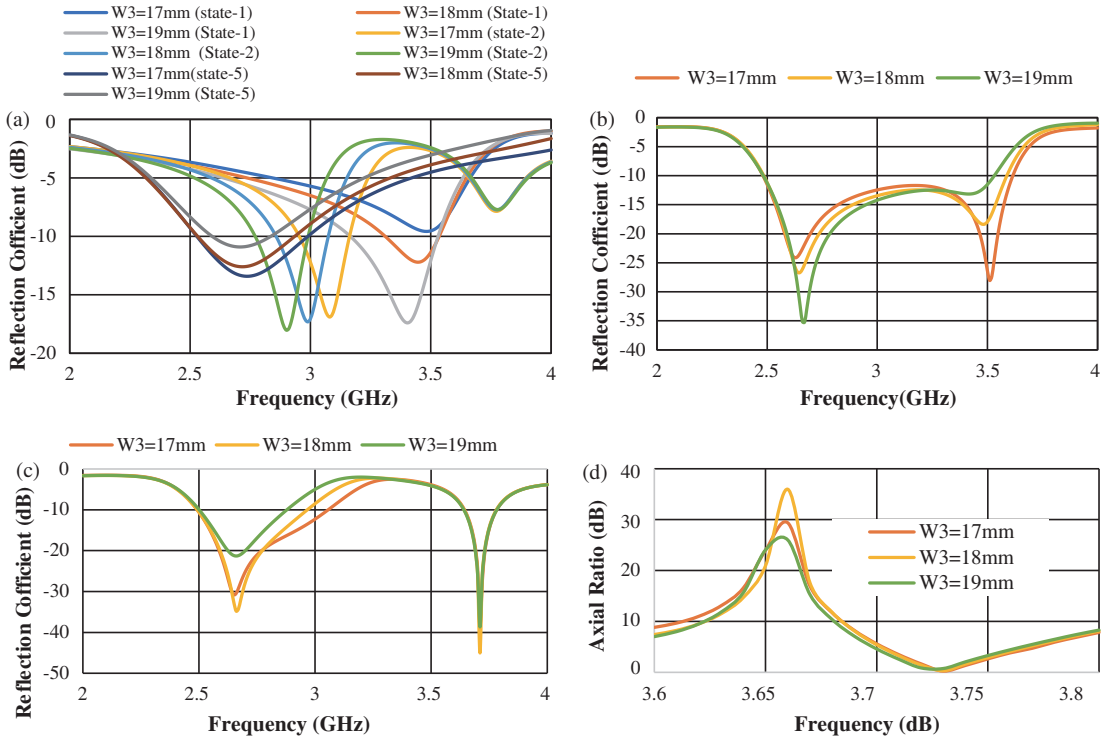

FIGURE 5. Variation in reflection coefficient (S_{11}) and axial ratio with $W3$.

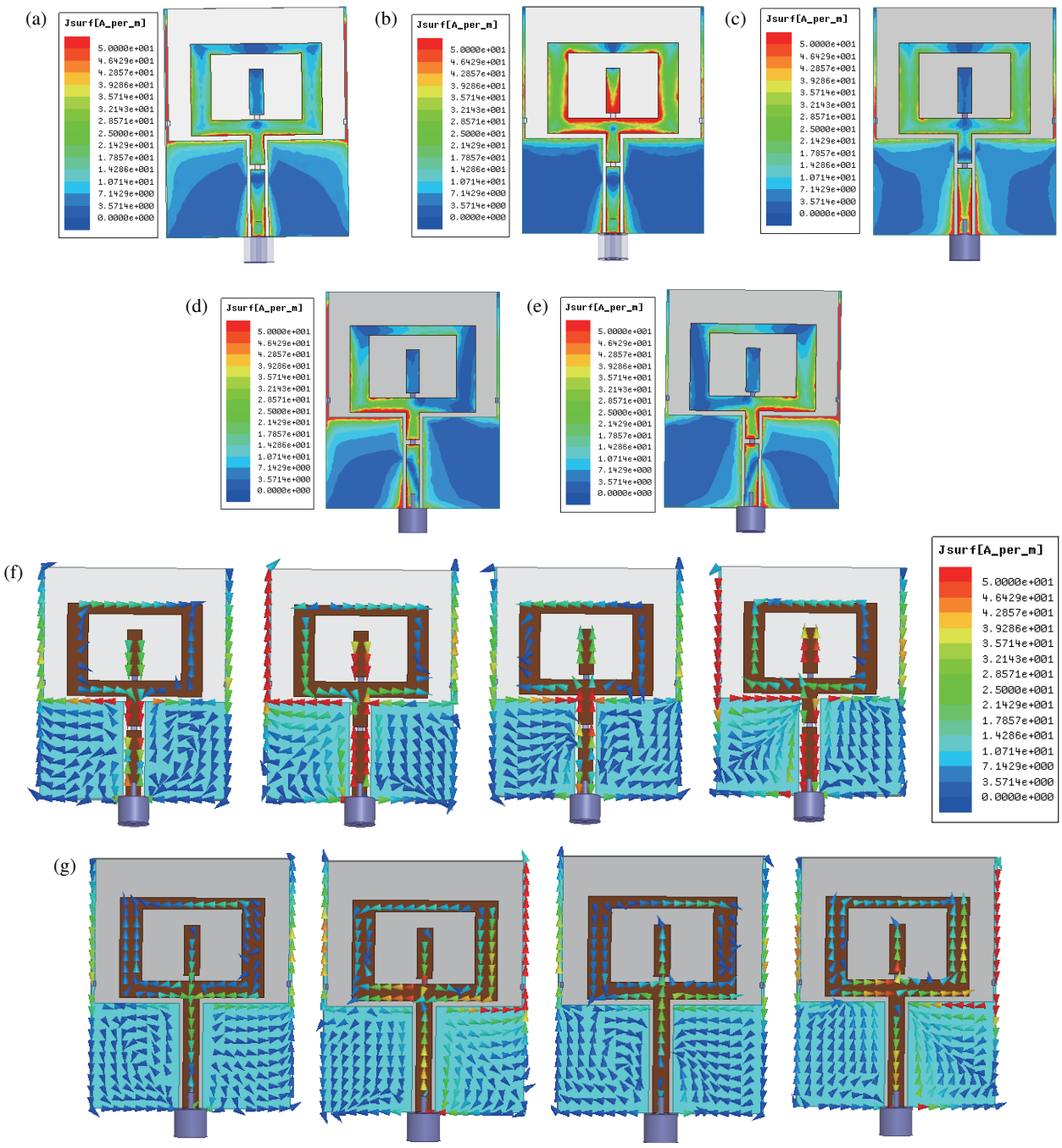

FIGURE 6. Current distributions at various states of operations. (a) State 1 (3.5 GHz). (b) State 2 (2.9 GHz), (c) State 5 (2.7 GHz). (d) State 3 (3.5 GHz), (e) State 4 (3.5 GHz). (f) Current distribution for state 6 (RHCP at 3.73 GHz). (g) Current Distribution for state 7 (LHCP at 3.73 GHz).

antenna via three RF-PIN diodes to obtain different reconfigurability conditions.

The suggested antenna is functional in seven states. Fig. 3(a) depicts the variation in the reflection coefficient (S_{11}) as a function of altering the diode states, and Fig. 3(b) shows the axial ratio attained at states 6 and 7.

Various states of operation by changing the condition of RF-PIN diodes are shown in Table 2.

2.3. Parametric Study

Table 1 displays the optimised dimensions of the suggested antenna. To obtain all three reconfigurable conditions — frequency, radiation pattern, and polarization — in the suggested antenna, a parametric study was carried out utilising a variety of parameters. It is found that in order to achieve polarisation reconfigurability in the suggested antenna, length $L3$ is a crucial element. Figs. 4(a) and (b) display the reflection coefficient and axial ratio performance at state 6. The symmetry causes the identical result to be seen in state 7. It has been noted that the ideal axial ratio is reached at $L3 = 9$ mm. $W3$ is an addi-

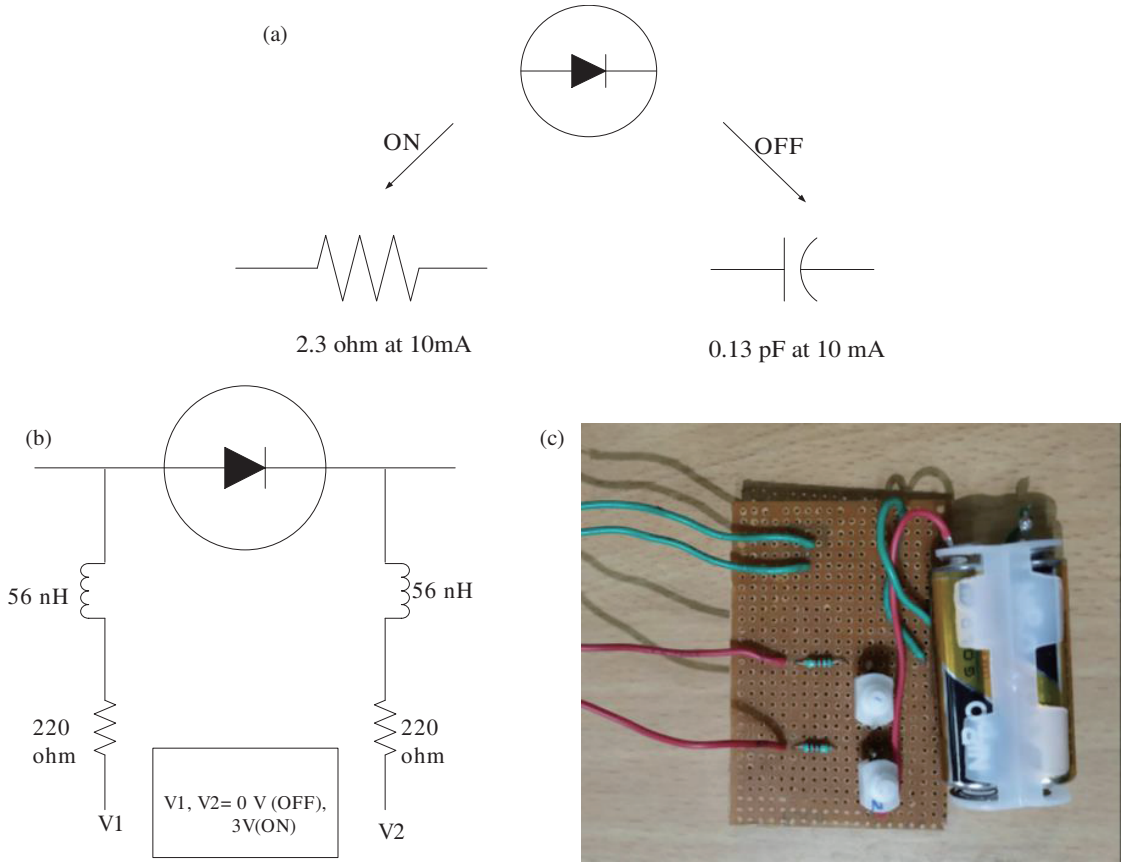

FIGURE 7. Equivalent value of RF-PIN diode BAR64-02V at OFF and ON state, (b) and (c) External biasing Circuit used for RF-PIN diode.

tional parameter that influences the intended antenna's performance. As seen in Figs. 5(a)–(c), the antenna's performance under various operating situations is observed. The variation in states 1, 2, and 5 is depicted in Fig. 5(a). It is noted that whereas impedance matching improves in state 1 as $W3$ grows, it does the opposite in state 5. It also has an impact on state 2's impedance matching, as seen in Fig. 5(a). The optimised outcome with $W3 = 18$ mm is taken into consideration. As observed in Figs. 5(b)–(d), $W3$ has no effect on the axial ratio in states 6 and 7 or the impedance matching of states 3, 4, 6, and 7.

2.4. Reconfigurability Principle

The proposed antenna is based on the concept of a switchable director/reflector [31]. This indicates that, with the aid of RF-PIN diodes, the two parasitic elements that are linked to the ground plane function as a director and a reflector, respectively, depending on their connection to the ground. The parasitic element connected to the ground functions as a reflector and the other element as a director while the $D1$ diode is in the ON state. The radiation pattern is orientated in the director's direction as a result of this effect. Two RF-PIN diodes are used in the suggested antenna to link the two parasitic elements to the ground plane. RF-PIN diode circumstances dictate that the radiation pattern is directed toward the director. In stages 3 and 4, pattern reconfigurability is attained. The size of the ground plane affects the current distribution when both parasitic elements are connected to or detached from it simultaneously. This effect leads to the achievement of frequency reconfigurability in states 1, and 5. To accomplish polarisation reconfigurability, an additional parasitic element is affixed to the rectangular ring antenna in the proposed antenna. The states that lead to polarisation reconfigurability are states 6 and 7. Fig. 6 displays the current distribution for every operational state.

As seen in Figs. 6(a), (b), and (c), the current is distributed symmetrically over the radiating structure in states 1, 2, and 5. As illustrated in Figs. 6(d) and (e), the current is distributed asymmetrically in the ground plane based on the ON/OFF conditions of the RF-PIN diodes and finds the directed radiation pattern in states 3 and 4. According to Figs. 6(f) and (g), in states 6 and 7 at a frequency of 3.73 GHz, the current is spread anticlockwise in state 6 to cause the right hand circular polarization (RHCP) condition to occur, and in state 7 to cause the left hand circular polarization (LHCP) condition to occur because current moves in clockwise direction, due to one parasitic element in the centre and one on the left and right sides, respectively.

2.5. Method for Switching

Numerous semiconductor switches have been employed in reconfigurable antennas. Semiconductor switches include varactor diodes, PIN diodes, and MEMS switches. Because of their

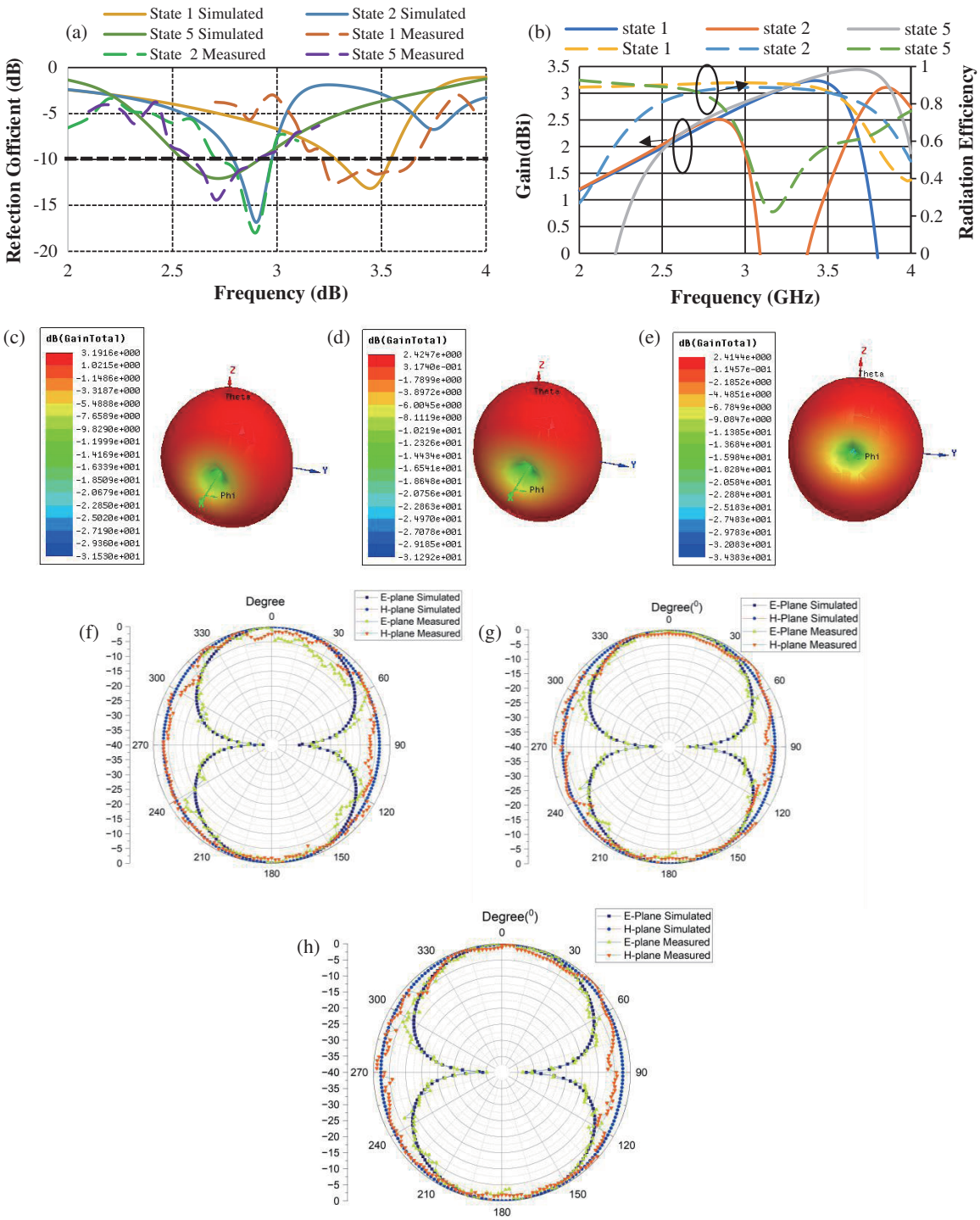

FIGURE 8. The Simulated and experimental results of proposed antenna in state 1, 2, and 5. (c) State 1 (3.5 GHz), (d) State 2 (2.9 GHz), (e) State 5 (2.7 GHz), (f) State 1 (3.5 GHz), (g) State 2 (2.9 GHz), (h) State (2.7 GHz).

strong isolation, fast switching, and low cost, RF-PIN diodes are the best choice for achieving complete reconfigurability in a single antenna [27]. The suggested circuit model for the RF-PIN diode BAR 64-02V [33], which is utilised in the suggested antenna layout, is depicted in Fig. 7(a). The RF-PIN diode provides 2.3-ohm resistance in the ON state and 0.13 pF capacitance in the OFF state, as illustrated in Fig. 7(a).

3. RESULT AND DISCUSSION

The electromagnetic (EM) full wave simulator HFSS Version 19.1 [32] is used to simulate the proposed antenna. As seen in Figs. 7(b) and (c), an external circuit is employed to bias the RF-PIN diodes. All of the suggested antenna's operational states are displayed in Table 2. An anechoic chamber is used for all measurements, including those of the axial ratio, radiation pattern, and reflection coefficient. There was a 5-met gap between

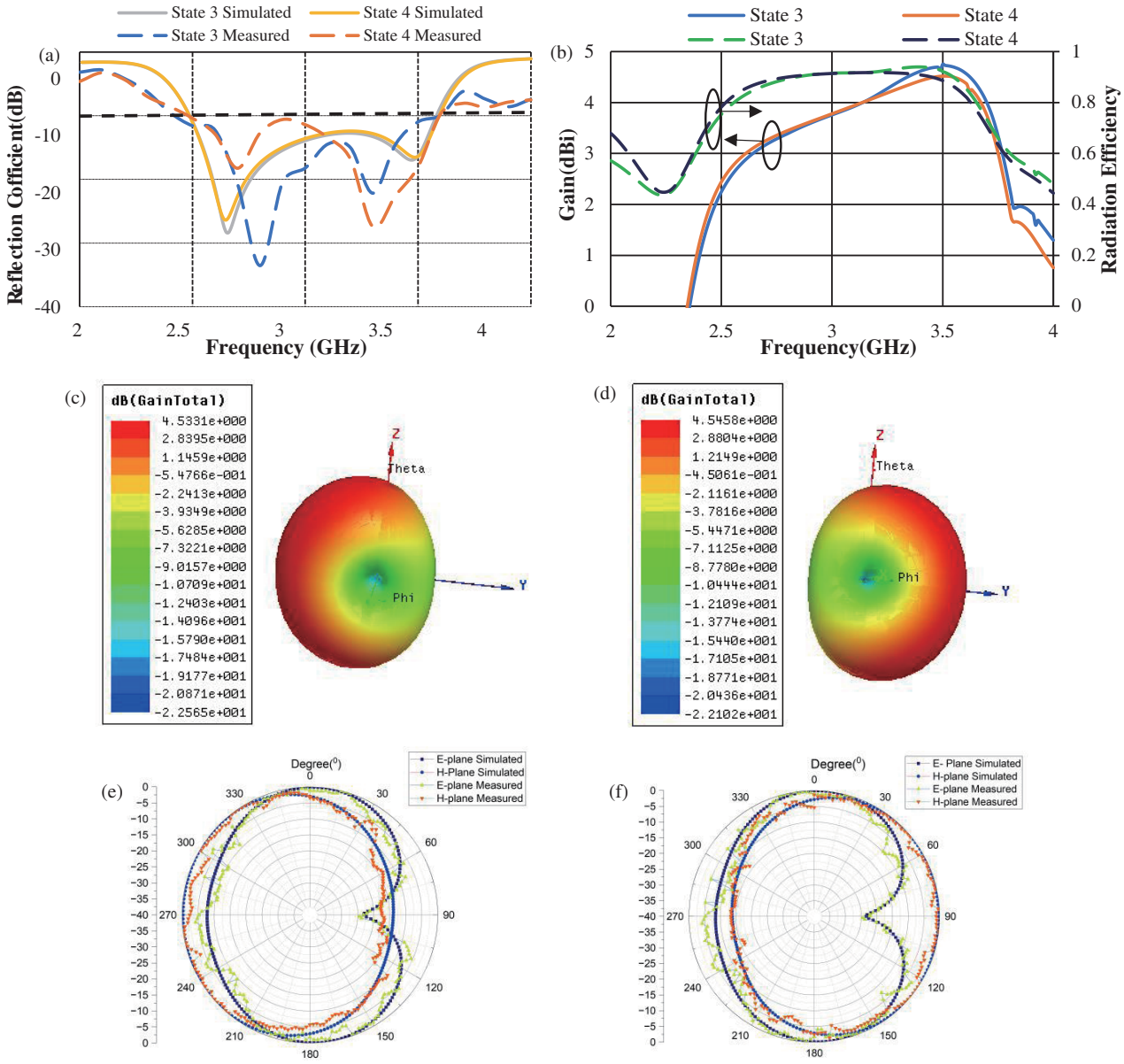

FIGURE 9. Simulated and experimental result of proposed antenna in state 3 and 4. (c) State 3 (3.5 GHz), (d) State 4 (3.5 GHz), (e) State 3 (3.5 GHz), (f) State 4 (3.5 GHz).

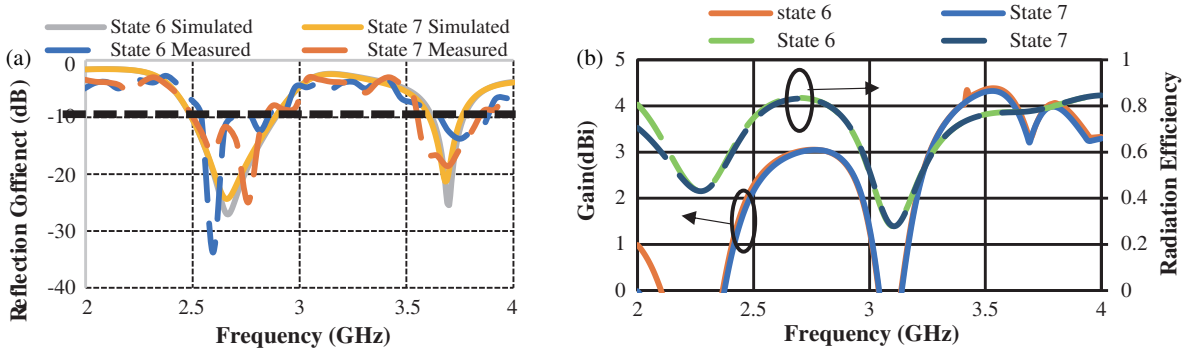

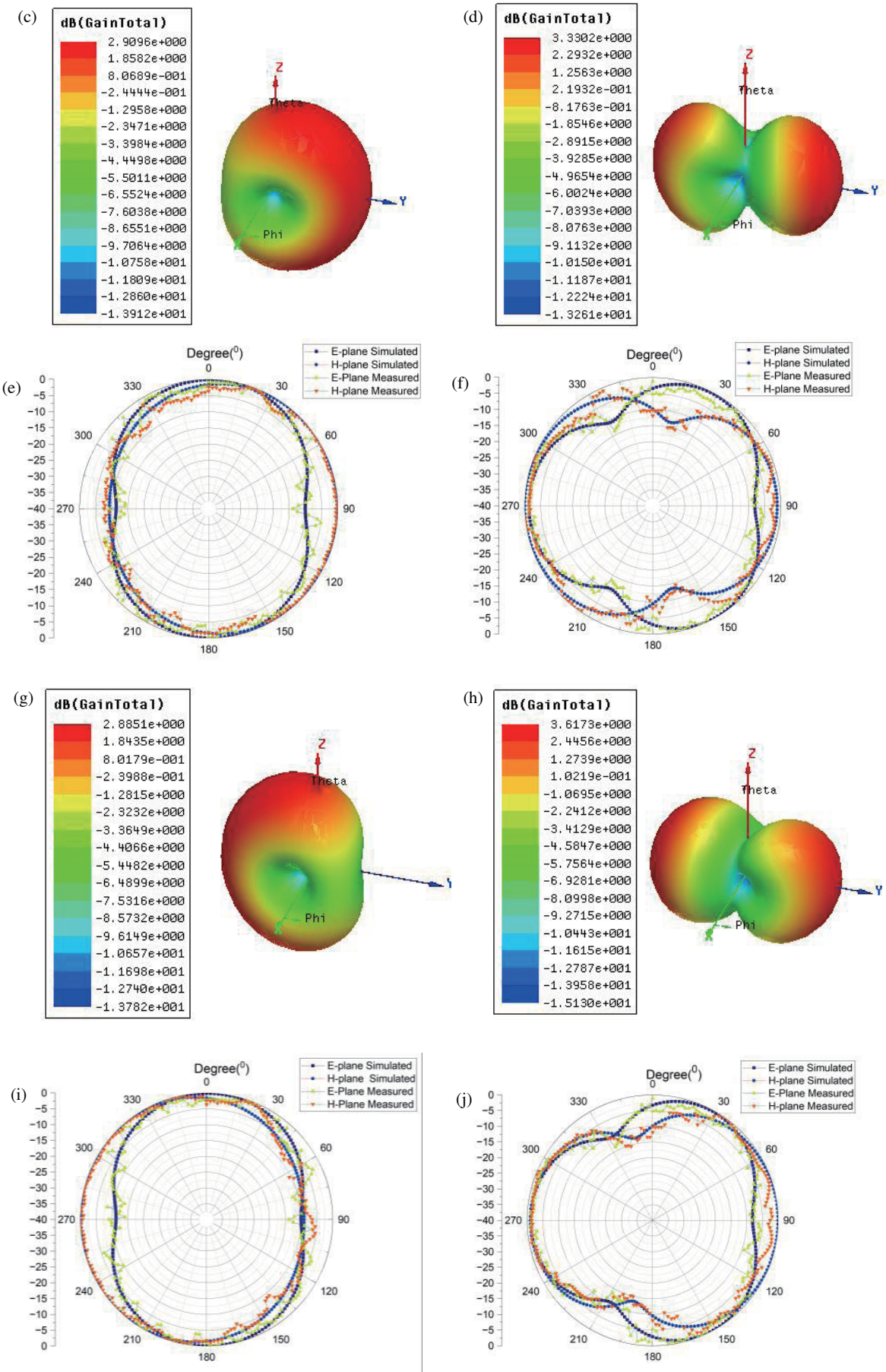
(c)
dB(GainTotal)
2.9096e+000
1.8582e+000
8.0689e-001
-2.4444e-001
-1.2958e+000
-2.3471e+000
-3.3984e+000
-4.4498e+000
-5.5011e+000
-6.5524e+000
-7.6038e+000
-8.6551e+000
-9.7064e+000
-1.0758e+001
-1.1809e+001
-1.2860e+001
-1.3912e+001
Z
Theta
Y
Phi
(d)
dB(GainTotal)
3.3302e+000
2.2932e+000
1.2563e+000
2.1932e-001
-8.1763e-001
-1.8546e+000
-2.8915e+000
-3.9285e+000
-4.9654e+000
-6.0024e+000
-7.0393e+000
-8.0763e+000
-9.1132e+000
-1.0150e+001
-1.1187e+001
-1.2224e+001
-1.3261e+001
Z
Theta
Y
Phi
(e)
Degree(0)
E-plane Simulated
H-plane Simulated
E-Plane Measured
H-plane Measured
(f)
Degree(0)
E-plane Simulated
H-plane Simulated
E-Plane Measured
H-plane Measured
(g)
dB(GainTotal)
2.8851e+000
1.8435e+000
8.0179e-001
-2.3988e-001
-1.2815e+000
-2.3232e+000
-3.3649e+000
-4.4066e+000
-5.4482e+000
-6.4899e+000
-7.5316e+000
-8.5732e+000
-9.6149e+000
-1.0657e+001
-1.1698e+001
-1.2740e+001
-1.3782e+001
Z
Theta
Phi
(h)
dB(GainTotal)
3.6173e+000
2.4456e+000
1.2739e+000
1.0219e-001
-1.0695e+000
-2.2412e+000
-3.4129e+000
-4.5847e+000
-5.7564e+000
-6.9281e+000
-8.0998e+000
-9.2715e+000
-1.0443e+001
-1.1615e+001
-1.2787e+001
-1.3958e+001
-1.5130e+001
Z
Theta
Y
Phi
(i)
Degree(0)
E-plane Simulated
H-plane Simulated
E-Plane Measured
H-Plane Measured
(j)
Degree(0)
E-plane Simulated
H-plane Simulated
E-Plane Measured
H-Plane Measured

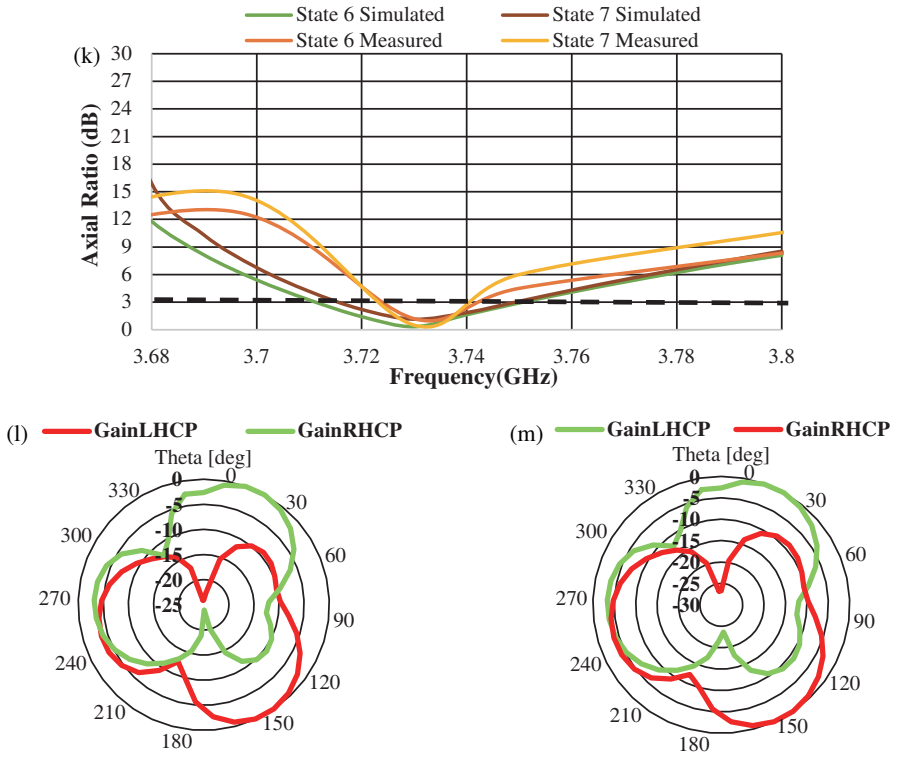

FIGURE 10. Simulated and experimental results of proposed antenna in state 6 and 7. (c) State 6 (2.67 GHz), (d) State 6 (3.73 GHz), (e) State 7 (2.67 GHz) (f) State 7 (3.73 GHz) (g) State 7 (2.67 GHz) (h) State 7 (3.73 GHz) (i) State 7 (2.67 GHz) (j) State 7 (3.73 GHz)

the source and the tested antenna. By varying the states of three RF-PIN diodes, the analysis of all seven states of operation can be simplified as follows.

3.1. Operating States 1, 2 and 5

The three RF-PIN diodes are all in the OFF state in state 1. In state 2, the other two diodes are in the OFF state, and only the D3 diode is in the ON state. Only D1 and D2 of the RF-PIN diodes are in the ON state in state 5, while D3 is in the OFF state. As seen in Figs. 6(a)–(c), in 1, 2, and 5 operating states, the current flows symmetrically in the radiating structure, and the radiation pattern is omnidirectional at frequencies of 3.5 GHz, 2.9 GHz, and 2.7 GHz, respectively.

Figure 8(a) displays both measured and simulated reflection coefficients. Figs. 8(c)–(e) depict the 3-D radiation patterns of states 1, 2, and 5, while Figs. 8(f)–(h) depict the simulated and measured 2-D radiation patterns in the E- and H-planes. As seen in Fig. 8(b), the peak gains in states 1, 2, and 5 are 3.18 dBi, 2.45 dBi, and 2.41 dBi, respectively, and the radiation efficiencies are 86%, 88%, and 86.7% observed.

3.2. Operating States 3 and 4

The suggested antenna covers a wide band frequency range from 2.47 to 3.57 GHz and gives the end-fire directed radiation pattern across the entire band when the RF-PIN diode, either D1 or D2, is ON, and D3 is OFF under both situations. This is because of the idea of the director and reflector, as seen in Figs. 9(c)–(d). Fig. 9(a) displays the measured and simulated reflection coefficients at states 3 and 4. Figs. 9(c)–(d) depicts the 3-D directed radiation patterns at 3.5 GHz in states 3 and 4. Figs. 9(e)–(f) show the measured 2-D radiation patterns at 3.5 GHz in the E- and H-planes. As illustrated in Fig. 9(b), the suggested antenna's peak gain in states 3 and 4 is 4.75 dBi, and its radiation efficiency is 92%.

3.3. Operating States 6 and 7

The proposed antenna provides the polarisation reconfigurability in operating states 6 and 7. Under these two circumstances, the RHCP is accomplished at a frequency of 3.73 GHz due to the asymmetric current distribution in the radiating structure in state 6, and LHCP occurs due to asymmetric current distribution in state 7. Because of the parasitic presence in the ground plane, the antenna resonates in the dual frequency bands of 2.49–2.75 GHz and 3.6–3.75 GHz, providing the direction radiation pattern. Fig. 10(a) displays the simulated and measured reflection coefficients of states 6 and 7. Figs. 10(c)–(d) and (g)–(h) depict the 3-D radiation patterns in states 6 and 7 at frequencies of 2.67 GHz and 3.73 GHz. Figs. 10(e)–(f) and (i)–(j) show the simulated and measured 2-D radiation patterns in the E-plane and H-plane at frequencies of 2.67 GHz and 3.73 GHz. As seen in Fig. 10(b), the radiation efficiencies are 82% and 78%, respectively, and the peak gains are 2.92 and 3.71 dBi. RHCP/LHCP polarisation reconfigurability is attained in states 6 and 7 at frequency 3.73 GHz. Fig. 10(k) shows both measured and simulated axial ratios under these two situations. Figs. 10(l) and 10(m) show the LHCP/RHCP gains in state 6 and 7. It is

TABLE 3. Comparative analysis of proposed antenna with existing antennas.

References	Dimensions (mm^3)	No. of layers/Copper layer	No. of switching Elements	Reconfigurability
[3]	$80 \times 80 \times 7.6$	Multi-layer	04	Frequency
[18]	$200 \times 83 \times 3.36$	Multi-layer	30	Frequency and Radiation Pattern
[22]	$35 \times 35 \times 1.6$	Double-sided copper layer	02	Frequency and Polarization
[24]	$25.56 \times 25.56 \times 1.6$	Double-sided copper layer	04	Frequency and Polarization
[26]	$60 \times 50 \times 1.6$	Double-sided copper layer	05	Frequency, Pattern and polarization
[27]	$36 \times 30 \times 1.6$	Double-sided copper layer	04	Frequency, Pattern and polarization
Proposed Antenna	$\mathbf{36 \times 45 \times 1.6}$	**Single-sided copper layer**	**03**	**Frequency, Pattern, and Polarization**

clearly observed that RHCP dominates in state 6, and LHCP dominates in RHCP.

Table 3 shows a comparative analysis of the proposed antenna with the existing reconfigurable antennas. The suggested antenna is single-layered and uses fewer diodes to achieve all reconfigurability properties and a wide range of applications.

4. CONCLUSION

This study introduces a single-layered CRA for 4G and 5G applications. This antenna offers three reconfigurable parameters: polarisation, radiation pattern, and frequency. With just three diodes, the proposed antenna has achieved such three-parameter reconfigurability. Three RF-PIN diodes are used to enable the seven distinct operating modes. It is observed that in radiation pattern reconfigurability, this antenna shows omni-directional, left-handed end-fire, and right-handed end-fire radiation patterns in a wide range of frequencies. Polarization reconfigurability is also achieved in LHCP/RHCP mode at a frequency range of 3.71–3.75 GHz. All states have good agreement between the simulated and measured results. The existence of lumped components causes some fluctuation in the outcome. This antenna is appropriate for all 4G and 5G applications since it uses the CPW feed for feeding purpose.

REFERENCES

[1] Gupta, A. and R. K. Jha, "A survey of 5G network: Architecture and emerging technologies," *IEEE Access*, Vol. 3, 1206–1232, 2015.

[2] Khan, T., M. Rahman, A. Akram, Y. Amin, and H. Tenhunen, "A low-cost CPW-fed multiband frequency reconfigurable antenna for wireless applications," *Electronics*, Vol. 8, No. 8, 900, 2019.

[3] Liu, T.-Y., J.-Y. Chen, and J.-S. Row, "Frequency reconfigurable antenna with dual-band and dual-mode operation," *Progress In Electromagnetics Research Letters*, Vol. 97, 115–120, 2021.

[4] Agarwal, S., A. Singh, and M. K. Meshram, "Frequency reconfigurable circular monopole antenna with key shaped ground stub," *Progress In Electromagnetics Research C*, Vol. 144, 127–135, 2024.

[5] Bharadwaj, S. S., D. Sipal, D. Yadav, and S. K. Koul, "A compact tri-band frequency reconfigurable antenna for LTE/Wi-Fi/ITS applications," *Progress In Electromagnetics Research M*, Vol. 91, 59–67, 2020.

[6] Saraswat, K. and A. R. Harish, "Flexible dual-band dual-polarised CPW-fed monopole antenna with discrete-frequency reconfigurability," *IET Microwaves, Antennas & Propagation*, Vol. 13, No. 12, 2053–2060, 2019.

[7] Chaouche, Y. B., F. Bouttout, M. Nedil, I. Messaoudene, and I. B. Mabrouk, "A frequency reconfigurable U-shaped antenna for dual-band WIMAX/WLAN systems," *Progress In Electromagnetics Research C*, Vol. 87, 63–71, 2018.

[8] Agarwal, S. and M. K. Meshram, "Pattern reconfigurable antenna using key-shaped monopoles for WiMAX application," in *2019 URSI Asia-Pacific Radio Science Conference (AP-RASC)*, 1–4, New Delhi, India, Mar. 2019.

[9] Agarwal, S. and M. K. Meshram, "CPW-fed wideband pattern reconfigurable antenna," in *2019 IEEE Indian Conference on Antennas and Propogation (InCAP)*, 1–4, Ahmedabad, India, Dec. 2019.

[10] Chen, S.-L., P.-Y. Qin, W. Lin, and Y. J. Guo, "Pattern-reconfigurable antenna with five switchable beams in elevation plane," *IEEE Antennas and Wireless Propagation Letters*, Vol. 17, No. 3, 454–457, Mar. 2018.

[11] Lim, I. and S. Lim, "Monopole-like and boresight pattern reconfigurable antenna," *IEEE Transactions on Antennas and Propagation*, Vol. 61, No. 12, 5854–5859, Dec. 2013.

[12] Zhao, S., Z. Wang, and Y. Dong, "A planar pattern-reconfigurable antenna with stable radiation performance," *IEEE Antennas and Wireless Propagation Letters*, Vol. 21, No. 4, 784–788, Apr. 2022.

[13] Lin, W., H. Wong, and R. W. Ziolkowski, "Wideband pattern-reconfigurable antenna with switchable broadside and conical beams," *IEEE Antennas and Wireless Propagation Letters*, Vol. 16, 2638–2641, 2017.

[14] Chen, Q., J.-Y. Li, G. Yang, B. Cao, and Z. Zhang, "A polarization-reconfigurable high-gain microstrip antenna," *IEEE Transactions on Antennas and Propagation*, Vol. 67, No. 5, 3461–3466, May 2019.

[15] Mak, K. M., H. W. Lai, K. M. Luk, and K. L. Ho, "Polarization reconfigurable circular patch antenna with a C-shaped," *IEEE Transactions on Antennas and Propagation*, Vol. 65, No. 3, 1388–1392, Mar. 2017.

[16] Panahi, A., X. L. Bao, K. Yang, O. O'Conchubhair, and M. J. Ammann, "A simple polarization reconfigurable printed monopole antenna," *IEEE Transactions on Antennas and Prop-*

agation, Vol. 63, No. 11, 5129–5134, Nov. 2015.

[17] Fartookzadeh, M. and S. H. M. Armaki, "Circular feeding network for circular polarisation reconfigurable antennas," *Electronics Letters*, Vol. 55, No. 12, 677–679, 2019.

[18] You, C. J., S. H. Liu, J. X. Zhang, X. Wang, Q. Y. Li, G. Q. Yin, and Z. G. Wang, "Frequency-and pattern-reconfigurable antenna array with broadband tuning and wide scanning angles," *IEEE Transactions on Antennas and Propagation*, Vol. 71, No. 6, 5398–5403, 2023.

[19] Li, J.-F., B. Wu, J.-Q. Zhou, K.-X. Guo, H.-R. Zu, and T. Su, "Frequency and pattern reconfigurable antenna using double layer petal shaped parasitic structure," *IEEE Transactions on Circuits and Systems II: Express Briefs*, Vol. 71, No. 4, 1934–1938, Apr. 2024.

[20] Rawal, P. and S. Rawat, "A novel S-shaped frequency and pattern reconfigurable patch antenna for 4G LTE, WLAN/Wi-Max application," *Microelectronics International*, Vol. 41, No. 1, 26–31, 2024.

[21] Selvam, Y. P., M. Kanagasabai, M. G. N. Alsath, S. Velan, S. Kingsly, S. Subbaraj, Y. V. R. Rao, R. Srinivasan, A. K. Varadhan, and M. Karuppiah, "A low-profile frequency-and pattern-reconfigurable antenna," *IEEE Antennas and Wireless Propagation Letters*, Vol. 16, 3047–3050, 2017.

[22] Vinayagam, K. and R. Natarajan, "Design of multiband frequency reconfigurable antenna with switchable polarization states," *Microwave and Optical Technology Letters*, Vol. 66, No. 2, e34057, 2024.

[23] Agarwal, S. and M. K. Meshram, "Low profile hybrid frequency and polarization reconfigurable bunny patch antenna for S-band applications," 2023.

[24] Monti, G., L. Corchia, and L. Tarricone, "Patch antenna with reconfigurable polarization," *Progress In Electromagnetics Research C*, Vol. 9, 13–23, 2009.

[25] Chen, A. and X. Ning, "A pattern and polarization reconfigurable antenna with metasurface," *International Journal of RF and Microwave Computer-Aided Engineering*, Vol. 31, No. 3, e22312, 2021.

[26] Selvam, Y. P., L. Elumalai, M. G. N. Alsath, M. Kanagasabai, S. Subbaraj, and S. Kingsly, "Novel frequency-and pattern-reconfigurable rhombic patch antenna with switchable polarization," *IEEE Antennas and Wireless Propagation Letters*, Vol. 16, 1639–1642, 2017.

[27] Ganesh, M., N. S. Raghava, T. Sabapathy, and Y. Sharma, "A compound reconfigurable electronically switched parasitic monopole antenna for sub 6 GHz wireless and vehicular applications," *AEU — International Journal of Electronics and Communications*, Vol. 179, 155335, 2024.

[28] Shanmuganantham, T., K. Balamanikandan, and S. Raghavan, "CPW-fed slot antenna for wideband applications," *International Journal of Antennas & Propagation*, 2008.

[29] Balanis, C. A., *Antenna Theory: Analysis and Design*, John Wiley & Sons, 2016.

[30] Pozar, D. M., *Microwave Engineering*, John Wiley & Sons, 2009.

[31] Alam, M. S. and A. M. Abbosh, "Wideband pattern-reconfigurable antenna using pair of radial radiators on truncated ground with switchable director and reflector," *IEEE Antennas and Wireless Propagation Letters*, Vol. 16, 24–28, 2016.

[32] Ansoft Corporation, Available at http://www.ansoft.com.

[33] Infineon Technologies, "Bar 64-02v," [online] Available: https://www.infineon.com/dgdl/Infineon-BAR64-02V.